The better heating rates presently computed using Scott's extrapolated values for γ_O are a result of the correct implementation of constant Prandtl number option in the VSL code and the axial grid sensitivity studies as mentioned earlier. It may be indicated here that apart from the requirement of extrapolation of the Scott's measured values (for lower Shuttle surface temperatures away from the stagnation region), surface heating predictions based on Scott's rates approach equilibrium levels (and the flight data) at lower altitudes (<55 km) slower as compared with those based on the present rates.

To evaluate the code independency of the present recombination-rate coefficients, surface heating rates have been calculated by employing these coefficients in another VSL code[11] (VSL3DNQ). Present predictions, as well as those from the code of Ref. 11, using the recombination rate expressions of Eqs. (3) and (4), are almost indistinguishable and in excellent agreement with the experimental data as shown in Fig. 3. This comparison provides a test to judge the applicability of present surface recombination rates with other flowfield codes. No effort has been made in this work to compare the present rates with the original rates of Kolodziej and Stewart[12] and Stewart et al.[13] Stewart has also recently reevaluated these rates, and his new results have not been published yet.

Concluding Remarks

Existing oxygen and nitrogen surface recombination coefficient expressions (obtained from heating data from the Shuttle flights) have been reevaluated in view of the corrections, changes, and grid resolution study carried out with a recently developed partially coupled VSL code. The changes include correcting code errors and incorporation of transport and thermodynamic properties from a recent study that are considered to be more accurate than the previous values. Similar to the earlier study, the new oxygen and nitrogen recombination-coefficient expressions are determined from the STS-2 surface heat-flux measurements at altitudes above 70 km along the windward symmetry plane. The current oxygen recombination-coefficient expression is shown to be more temperature dependent than the previous expression. Quite good comparison is obtained between the predicted and measured heating values over the range of STS-2 entry conditions from approximately 78 to 61 km altitude. The previous recombination coefficient values result in larger heat-flux predictions as compared with the flight data, with a maximum difference of about 20% at an altitude of 60.56 km.

Acknowledgments

The author would like to thank K. P. Lee for help in obtaining the present results and R. A. Thompson for the VSL3D results used for comparison. E. V. Zoby provided helpful suggestions during the preparation of this manuscript.

References

[1]Zoby, E. V., Gupta, R. N., and Simmonds, A. L., "Temperature-Dependent Reaction Rate Expressions for Oxygen Recombination," *Thermal Design of Aeroassisted Orbital Transfer Vehicles*, edited by H. F. Nelson, Vol. 96, Progress in Astronautics and Aeronautics, AIAA, New York, 1985, pp. 445–464.

[2]Shinn, J. L., Moss, J. N., and Simmonds, A. L., "Viscous-Shock-Layer Heating Analysis for the Shuttle Windward Plane with Surface Finite Catalytic Recombination Rates," *Entry Vehicle Heating and Thermal Protection Systems: Space Shuttle, Solar Starprobe, Jupiter Galileo Probe*, edited by P. E. Bauer and H. E. Collicott, Vol. 85, Progress in Astronautics and Aeronautics, AIAA, New York, 1983, pp. 149–181.

[3]Lee, K. P., and Gupta, R. N., "Viscous-Shock-Layer Analysis of Hypersonic Flows Over Long Slender Vehicles," NASA CR-189614, March 1992.

[4]Lee, K. P., "Viscous-Shock-Layer Analysis of Hypersonic Flows Over Slender Vehicles," Ph.D. Thesis, Dept. of Mechanical Engineering and Mechanics, Old Dominion Univ., Norfolk, VA, Aug. 1988.

[5]Gupta, R. N., Lee, K. P., and Zoby, E. V., "Enhancements to Viscous-Shock-Layer Technique," AIAA Paper 92-2897, July 1992.

[6]Moss, J. N., "Reacting Viscous-Shock-Layer Solutions with Multicomponent Diffusion and Mass Injection," NASA TR R-411, June 1974.

[7]Gupta, R. N., Yos, J. M., Thompson, R. A., and Lee, K. P., "A Review of Reaction Rates and Thermodynamic and Transport Properties for an 11-Species Air Model for Chemical and Thermal Nonequilibrium Calculations to 30000 K," NASA RP-1232, Aug. 1990.

[8]Engel, C. D., Farmer, R. C., and Pike, R. W., "Ablation and Radiation Coupled Viscous Hypersonic Shock Layers," NASA CR-112306, Sept. 1971.

[9]Esch, D. D., Siripong, A., and Pike, R. W., "Thermodynamic Properties in Polynomial Form for Carbon, Hydrogen, Nitrogen, and Oxygen Systems from 500 to 15000 K," NASA CR-111989, Nov. 1970.

[10]Scott, C. D., "Catalytic Recombination of Nitrogen and Oxygen on High-Temperature Reusable Surface Insulation," *Aerothermodynamics and Planetary Entry*, edited by A. L. Crosbie, Vol. 77, Progress in Astronautics and Aeronautics, AIAA, New York, 1981, pp. 192–213.

[11]Swaminathan, S., Kim, M. D., and Lewis, C. H., "Three-Dimensional Nonequilibrium Viscous Shock-Layer Flows over Complex Geometries," AIAA Paper 83-0212, Jan. 1983.

[12]Kolodziej, P., and Stewart, D. A., "Nitrogen Recombination on High-Temperature Reusable Surface Insulation and the Analysis of its Effect on Surface Catalysis," AIAA Paper 87-1637, June 1987.

[13]Stewart, D. A., Chen, Y. K., and Henline, W. D., "Effect of Nonequilibrium Flow Chemistry and Surface Catalysis on Surface Heating to AFE," AIAA Paper 91-1373, June 1991.

T. C. Lin
Associate Editor

Effect of Transpiration Cooling on Nozzle Heat Transfer

F. Chen,* W. J. Bowman,† and R. Bowersox‡
U.S. Air Force Institute of Technology, Wright–Patterson Air Force Base, Ohio 45433-7755

Introduction

RENEWED interest in liquid propellant space launch vehicles has sparked research to improve the performance of these systems.[1] Nozzle heat transfer and material thermal limitations remain limiting factors in the performance of modern rocket engines. Actively cooled rocket nozzles allow the high-combustion temperatures necessary for high performance while maintaining the structural integrity of the nozzle. Several methods of active cooling have been employed to address this problem, including regenerative, film, and transpiration cooling.

Regenerative cooling involves pumping a liquid through channels surrounding the outside of the combustion chamber. Film cooling involves injecting gas or liquid through one or several discrete holes in a nozzle wall to establish a protective film on the surface. Transpiration cooling is essentially the limiting case of film cooling because it involves pushing gas or liquid uniformly through an area of porous wall material.[2] Ideally, it can be thought of as an infinite number of film cooling ports with zero distance between them. This cooling has been successfully used for cooling injector faces in the upper stage engine (J-2) of the moon launch vehicle and the Space Shuttle main engines, but it has not been used for cooling the thrust chamber or nozzle regions of large rocket engines.[2]

It is expected that a heat transfer rate reduction similar to or better than film cooling can be realized with decreased flow disturbances, indicating that transpiration cooling could be a more attractive method than film or regenerative cooling. Therefore, this investigation proposes to study the effects of transpiration cooling in a supersonic nozzle on heat transfer. Compared to an earlier study,[1] a wider range of blowing ratios were examined.

The objective of this research was to investigate the differences between flow over a porous wall with blowing and a nonporous wall with no blowing. In particular, the effect of blowing ratio on the nozzle heat transfer characteristics were studied. These objectives

Received Oct. 23, 1995; revision received Dec. 13, 1995; accepted for publication Dec. 20, 1995.

*Research Assistant, Aero/Astronautical Engineering Department.

†Associate Professor, Aero/Astronautical Engineering Department. Senior Member AIAA.

‡Assistant Professor, Aero/Astronautical Engineering Department. Member AIAA.

were accomplished with a shock tube study of a two-dimensional, Mach 2.0 [exit Reynolds number per meter ($Re = 5.2 \times 10^7$/m)] nozzle, where one of the nozzle walls was constructed from porous material. The sintered steel (porous) portion of the nozzle contour started just upstream of the nozzle throat (see Fig. 1 for a schematic of the present model) and used air as the primary and injected fluid.

Experimental Apparatus

More details about the facilities, model, and instrumentation can be found in Ref. 1. The model used for this experiment was a two-dimensional, Mach 2.0 method of characteristics contoured nozzle, Fig. 1 (exit $Re = 5.2 \times 10^7$/m). One side of the nozzle was modified for blowing while the other remained solid (the nonblowing side).

Four layers of 1.59-mm-thick 316L sintered stainless steel made from 2.0-μm beads were installed on the blowing side of the nozzle. The porous material started 1.3 cm upstream of the throat and extended to 1.2 cm downstream of the throat. The size of the blowing region was different from the work of Keener et al.,[1] who performed a test with a similar nozzle that allowed for blowing along the entire diverging section of the nozzle wall. Each layer of porous material was shaped to the nozzle individually to minimize unevenness where the porous material met the solid nozzle wall. A plenum chamber was used to supply the injectant gas for the porous nozzle wall (see Fig. 1).

The run times in the shock tube were very short ($\approx$1.5 ms); hence, high-frequency response pressure transducers and heat flux gauges were required for data collection. Pressure transducers and heat flux gauges were placed in pairs along the nozzle walls. Also, pressure transducers were placed in the injection plenum and along the top of the shock tube upstream of the nozzle. See Fig. 1 for the instrumentation locations.

Eight blowing ratios were investigated during this experiment. The plenum pressure was used to control the blowing ratio. The local blowing ratio, which represented the total averaged injection to nozzle exit mass flow rate, was defined as

$$B_s = \frac{1}{\rho_\infty u_\infty t} \int_0^s (\rho_i u_i)\, ds \tag{1}$$

where ρ is density, u velocity, t nozzle height at the location of interest, and s distance along the blowing region. The subscript i is for the injectant gas, where ∞ is the stream free condition. The injectant mass flow rate was determined from the manufactures mass flow rate-pressure drop chart.[3] The chart was verified for the present experiment.

At the lower gas-injection pressures, the possibility existed for the pressure in the nozzle to be greater than the gas-injectant pressure, especially upstream from the nozzle throat where the nozzle static pressure was greatest. This would result in suction in the upstream portion of the nozzle. As the nozzle pressure dropped below the gas injection pressure, positive injection was observed. As a result, both positive and negative blowing ratios were studied.

Heat-flux gauges (more accurately referred to as thin-film resistance thermometers) were used to measure variations in surface temperature through changes in the resistance of the thin film. The surface temperature history was then used to determine heat transfer to the surface of a gauge. If both the substrate of the gauge is assumed to be a semi-infinite slab and the film of platinum assumed to be so thin that it does not affect the temperature history of the surface of the substrate, then the relation between the temperature history of the gauge and the heat flux imparted to the surface can be obtained[4]:

$$q''(t) = \sqrt{\frac{\rho c k}{\pi}} \left[\frac{T(t)}{\sqrt{t}} + \frac{1}{2} \int_0^t \frac{T(t) - T(\tau)}{(t-\tau)^{\frac{3}{2}}}\, d\tau \right] \tag{2}$$

where the parameter $\sqrt{(\rho c k)}$ is called the thermal product. The thermal product of each gauge was found during a calibration experiment.

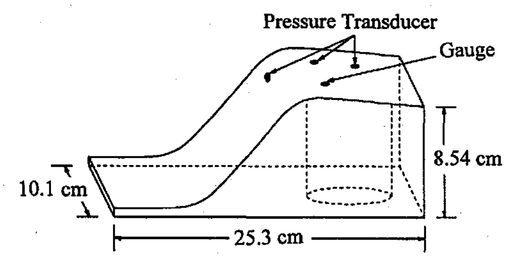

Nonblowing side view

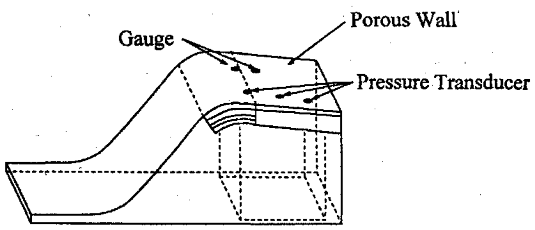

Blowing side view

Fig. 1 Schematic of Mach 2.0 contoured nozzle with a sintered stainless steel floor.

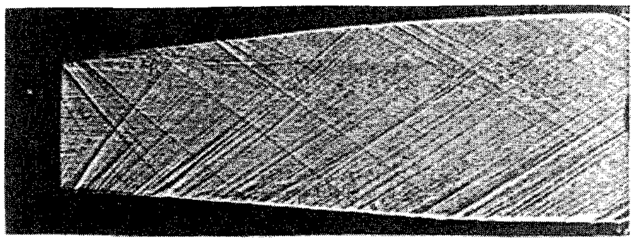

a) Blowing ratio BR = 0

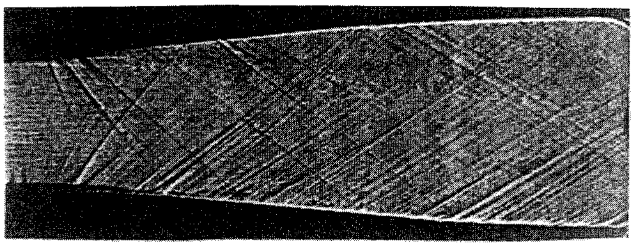

b) Blowing ratio BR = 0.002

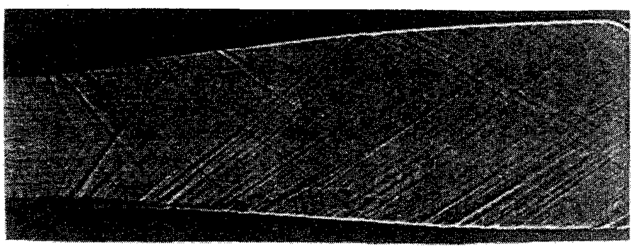

c) Blowing ratio BR = 0.0056

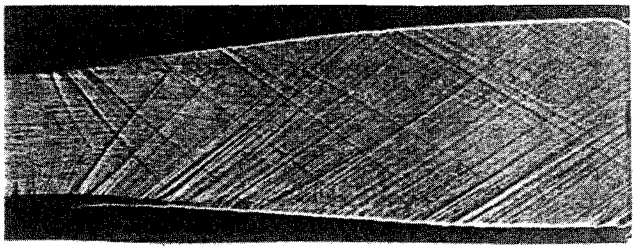

d) Blowing ratio BR = 0.0112

Fig. 2 Shadowgraphs, boundary-layer effects with blowing (blowing along lower wall).

These temperature data were numerically integrated using the relationship[5]

$$q''(t_J) = 2\sqrt{\frac{\rho c k}{\pi}} \sum_{j=1}^{J} \frac{T(t_j) - T(t_{j-1})}{\sqrt{t_J - t_j} + \sqrt{t_J - t_{j-1}}} \tag{3}$$

The present data were found to be repeatable to within about 10%.

Results and Discussion

The nonblowing side of the nozzle provided reference heat-flux data (no transpiration cooling) throughout the testing. It was assumed that the effects of blowing on one wall would not significantly effect the boundary layer on the other wall. This assumption seems reasonable for the low blowing ratios used in the present study.

Shadowgraph visualization of the boundary layer at each blowing level was the first indication that transpiration cooling had an effect on the boundary layer. Figure 2 shows a series of shadowgraphs for each blowing level. Notice that the boundary layer on the nonblowing wall appears to be unaffected by blowing for all of the test cases. This result supports the assumption concerning the usage of the opposite wall nonblowing data as a comparison. The heat flux results are plotted against the blowing ratio in Fig. 3. As can be seen, for the lowest total blowing ratios, some of the gauges were located in a region of negative blowing ratio. A curve fit for the data from zero blowing ratio to blowing ratio 0.0117 was obtained and can be expressed as

$$h/h_0 = 0.94\exp(-43B_s) \qquad (B_s < 0.0117) \tag{4}$$

where h_0 is the nonblowing side turbulent heat transfer coefficient.[6] Figure 3 also contains the data from Ref. 1. Good agreement between the data can be seen.

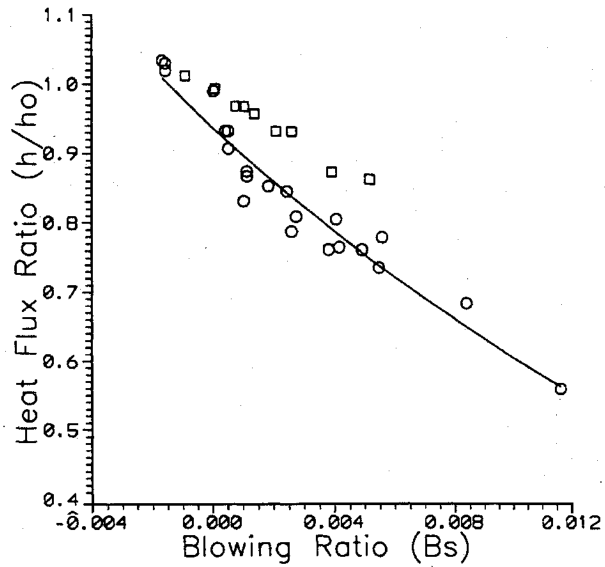

Fig. 3 Blowing effects on heat transfer coefficient: ○, experimental data; □, Keener et al.[1]; and curve fit: $h/h_0 = 0.94\exp(-43B_s)$.

The flow in the nozzle throat region is believed to be turbulent. This is based on the nozzle exit Reynold's number, which was 5.2×10^7/m. The effect of wall roughness resulting from the porous wall on the turbulent boundary layer was studied in detail by Keener.[1] The shadowgraph photos (Fig. 2) indicate that boundary-layer growth on the rough and smooth walls was similar.

Conclusions

The effects of transpiration cooling at various blowing ratios on turbulent heat transfer were investigated on a two-dimensional contoured nozzle. Overall, the heat transfer rate was shown to be significantly reduced by transpiration cooling. A 40% reduction was measured for a local blowing ratio of 1.17%. The present two-dimensional results have indicated that transpiration cooling has the potential to be an effective means of rocket nozzle cooling.

References

[1]Keener, D., Lenertz, J., Bowersox, R., and Bowman, J., "Transpiration Cooling Effects on Nozzle Heat Transfer and Performance," *Journal of Spacecraft and Rockets*, Vol. 32, No. 6, 1995, pp. 981–985.

[2]Sutton, G. P., *Rocket Propulsion Element*, 6th ed., Wiley, New York, 1992, pp. 289–294.

[3]Anon., "Technical Handbook for Precision Porous Metal Products," Mott Metullurgical Corp., Product Catalog No. 1000A, Farmington, CT, 1986.

[4]Schultz, D., and Jones, T., "Heat Transfer Measurements in Short Duration Hypersonic Facilities," AGARDograph, AGARD-AG-165, Feb. 1973.

[5]Cook, W., and Felderman, E., "Reduction of Data from Thin-Film Heat-Transfer Gages: A Concise Numerical Technique," *AIAA Journal*, Vol. 4, No. 3, 1966, pp. 561, 562.

[6]Bartz, D. R., "A Simple Equation for Rapid Estimation of Rocket Nozzle Convective Heat Transfer Coefficients," *Jet Propulsion*, Vol. 27, No. 1, 1957, pp. 49–51.

J. C. Adams
Associate Editor